International Conference on Green Energy and Environmental Engineering(GEEE-2017)
International Journal of Control, Energy and Electrical Engineering - CEEE
Vol.4 pp. 60-65

Fault detection of the photovoltaic system by artificial neural networks

C. Karamostefa khelil[#1], K. Kara[*2], A. Chouder[#3].

[#]*Set laboratory, Electrical engineering Department, Blida1 University*
BP 270, Blida 09000, Algeria
[1]c.karamostefa@univ-blida.dz
[3]k.kara@yahoo.fr

[*]*Electrical Engineering Department, Faculty of Technology, M'Sila University,*
BP 166 Ichbilia, M'Sila 28000, Algeria
[2]aissachouder@yahoo.fr

***Abstract*— This article proposes the modelling, detection and classification of the faults of a grid connected photovoltaic system by artificial neural networks. The validation of our study required a real meteorological data such as (Module Temperature, Solar Irradiance) as well as electrical data (Impp, Vmpp) of the month of March 2014, the system is composed of sixteen Photovoltaic modules connected to network of the station CDER in Algiers, Algeria. The fault detection algorithm compares the measured and the simulated data by artificial neurons mentioned above, using the percentage of linearity ratio method. The system proved a good efficiency between the measured and the simulated values as well as the remarkable results of the detection algorithm.**

***Keywords*—Photovoltaic system; Artificial neural network; Modelling; detection; Classification.**

I. INTRODUCTION:

Renewable energies are derived from inexhaustible natural resources such as water, earth heat, wind, and solar. In many countries, these energies have been developed considerably and particularly solar energy, which proves that solar irradiance is the greatest source of energy now a days.

Photovoltaic solar system consists of generating power from light through photovoltaic cells, it is used widely to power orbit satellites and electrical equipment in isolated sites. In the industrialized countries, photovoltaic power installations have also been connected to electricity distribution networks.

The global cumulative photovoltaic capacity has increased exponentially worldwide up to 177GW by the end of 2014. [1] This growth indicates that photovoltaic energy production will have a very important role in the production of electricity in the future.

Many factors can influence PV energy loss, such as aging along with loss of wiring connection [2], loss of shading [3], dust or snow accumulation on PV modules [4], MPPT error [5,6], the failures of the DC-AC inverter [7,8].

There are present techniques which were developed for fault detection in GCPV systems. Some of these methods requires no meteorological data (temperature, irradiance) such as the earth capacity measurements [9]. However others uses those meteorological and satellite data for fault prediction [15].

Different fault detection techniques are based on threshold diagnosis method which detect faults in a GCPV plant [10], In addition other methods proposed a reliable fault detection method [11,12], where the system depends not only on actual meteorological data (Module Temperature , Solar Irradiance) but also other parameters such as DC input / output ratio, AC input / output and a measured reference efficiency.

Faults such as partial shadow, shadowing effect with faulty bypass diodes, another type of shading effect with lost connection can be detected with different monitoring platforms as virtual instrumentation LabVIEW [15]. Other algorithms used are based on artificial intelligence techniques like ANN [13] and fuzzy logic [14]

In this study we propose the modelling, the detection and the classification of the faults by ANN passing by:

- The selection of the ANN architecture for the validation of (Impp, Vmpp) from meteorological data (Module Temperature, Solar Irradiance) called the modelling phase.
- Fault detection by ANN to identify the actual measured with the simulated data from the modelling phase.
- Algorithm of classification using the percentage of linearity ratio.

II. DESCRIPTION OF THE DATA ACQUISITION ON GCPV PLANT

The PV used in this study is a connected system to the network of the photovoltaic station at CDER. It consists of a generator of 16 monocrystalline photovoltaic modules of ISOFOTON type with peak power 106W and nominal voltage of 12V. The 16 modules are made up of two parallel branches. Each branch contains 8 modules connected in series. This generator is connected to a power conditioning device: it consists of a DC / DC converter mainly for tracking of the maximum power point (MPPT) and of a DC / AC converter to adapt the characteristics of the energy produced by the PV generator to the electrical network. The system is protected by

ISSN 2356-5608

differential circuit breaker, magneto-thermal and varistor breaker; Then the reversible counter which rotates in two directions, one for consumption, and the other for production. At the end injected to the low voltage electrical distribution network: 220V-50 Hz.

The monitoring is particularly based on key variables. Therefore a system must be developed to allow the acquisition and transfer of variables affecting the system as irradiance, temperature and the output generated data (current and voltage). The different elements used in the acquisition system are shown in the figure 1.

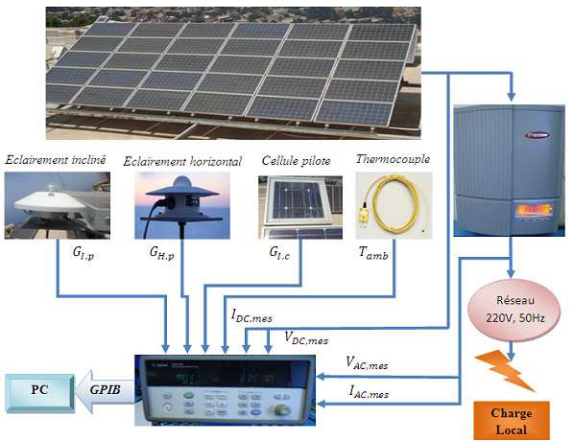

Fig. 1. Overview of the global acquisition system

The electrical characteristics of the photovoltaic module used under standard conditions (Temperature Module = 25 ° C, Solar Irradiance = 1000W / m2) are shown in Table 1:

TABLE I
ELECTRICAL CHARACTERISTICS OF THE PV MODULE

Parameters	Values
Short circuit Isc0 at STC	6.54 A
Open Circuit Vco0 at STC	21.6 V
Current Pmpp0 at STC	6.1 A
Voltage Pmpp0 at STC	17.4 V
Pmpp0 at STC	106 W
Resistor Rs	0.149Ω
Resistor Rsh	200Ω

III. FAULTS IN THE PHOTOVOLTAIC GENERATOR

The faults encountered in a photovoltaic system are mainly related to photovoltaic generators, inverters, storage systems and power grids. This work aims to detect the faults occurring in the photovoltaic network shown in Table 2, with their references:

TABLE II
DIFFERENT TYPE OF FAULTS AND THEIR SYMBOLS

Name of Faults	Symbol
Normal operation	C1
Fault detection refer to one panel short circuit	C2
Fault detection refer to four panels short circuit	C3
Fault detection refer to string	C4

IV. METHODOLOGY

A. *DC Output Modeling*

The modeling of the GCPV to DC system requires a parameter model, defined by the Newton-Raphson equation [16] (1):

$$I = Iph - I_0\left(exp\frac{q(V+R_SI)}{nkT_c} - 1\right) - \frac{V+IR_S}{R_p} \quad (1)$$

Where:
Iph: photo generated current at STC,
Rs: cell series resistance,
Rp: cell parallel resistance,
Tc: Temperature of the cell,
K: constant of Boltzmann (1.38 x 10^{-23} J/°K),
q: charge of the electron (1.6 x 10^{-19} C),
I_0: saturation current at STC.
N: the diode ideality factor.

B. *Fault detection*

The main purpose of fault detection in a system is to detect and determine when and where an error has occurred in a grid-connected photovoltaic installation as shown in general algorithm figure 2.

The fault diagnosis algorithm is based on the percentage of linearity ratio between the mean of the measured values and the mean of the simulated values by artificial neural network of the normal operations model, the percentage of linearity ratio will be applied separately on both variables Impp and Vmpp shown in the equation (2, 3), if the value of the percentage ratio of the variables (Impp, Vmpp) is about 100%; Implies that the system is normal operation.

For the good precision, the percentage of linearity ratio must be limited between the minimum and the maximum value. The linear regression line is applied and calculated by the least squares method, both coefficient a,b of are determined in the equation (4, 5).

$$\alpha_{(\min,\max)} = \frac{\frac{1}{n}\cdot\sum_{i=1}^{n} I_{mppmeas(\min,\max)}}{\frac{1}{n}\cdot\sum_{i=1}^{n} I_{mppsim(\min,\max)}}.100 \quad (2)$$

$$\beta_{(\min,\max)} = \frac{\frac{1}{n}\cdot\sum_{i=1}^{n} V_{mppmeas(\min,\max)}}{\frac{1}{n}\cdot\sum_{i=1}^{n} V_{mppsim(\min,\max)}}.100 \quad (3)$$

$$a = \frac{(n*\sum_{i=1}^{n} Imppsim*Imppmeas - \sum_{i=1}^{n} Imppsim*\sum_{i=1}^{n} Imppmeas)}{(n*\sum_{i=1}^{n}(Imppsim)^2 - (\sum_{i=1}^{n} Imppsim)^2)} \quad (4)$$

$$b = (1/n) * (\sum_{i=1}^{n} Imppmeas - a * \sum_{i=1}^{n} Imppsim) \quad (5)$$

Where:
(α, β) min: Minimum percentage of linearity ratio of the Impp, Vmpp respectively under the linear regression line.
(α, β) max: Maximum percentage of linearity ratio of the Impp, Vmpp respectively on the linear regression line.
Imppmeasmin: Minimum measured current at maximum power point.
Imppsimmin: Minimum simulated current at maximum power point.
Imppmeasmax: Maximum measured current at maximum power point.
Imppsimmax: Maximum simulated current at maximum power point.
Vmppmeasmin: Minimum measured voltage at maximum power point.
Vmppsimmin: Minimum simulated voltage at maximum power point.
Vmppmeasmax: Maximum measured voltage at maximum power point.
Vmppsimmax: Maximum simulated voltage at maximum power point.
n: Number of samples.

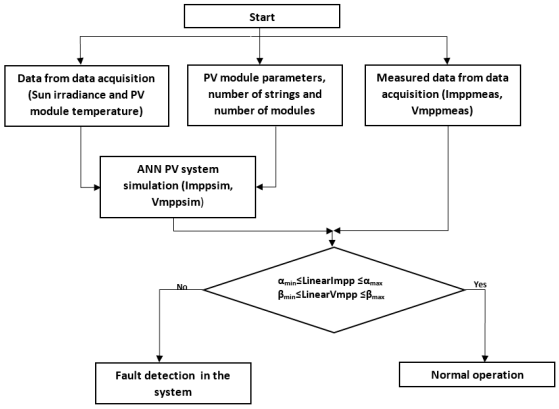

Figure 2. General algorithm using percentage of linearity ratio for detection

ISSN 2356-5608

C. *Combination of attributes*

Each class of (Impp, Vmpp) variables contains an identification symbol shown in Table 3:

TABLE IIIII
IMPP, VMPP IDENTIFICATION SYMBOLS

Symbols	Description	Classes
Imppn	Normal operation maximum power point current	C1I
Imppstring	Maximum power point current of faulty string	C2I
Vmppn	Normal operation maximum power point voltage	C1V
Vmpp1sc	Maximum power point voltage of one module short circuited	C2V
Vmpp4sc	Maximum power point voltage of four modules short circuited	C4V

The classification of various faults can be made from the combination between the two variables Impp and Vmpp shown in Table 4:

TABLE IVV
IMPP, VMPP COMBINATION FAULT IDENTIFICATION

Impp	Vmpp	System description
Imppn	Vmppn	Normal operation
Imppn	Vmpp1sc	One faulty PV module short circuit in string
Imppn	Vmpp4sc	Four faulty PV modules short circuit in string
Imppstring	Vmppn	Faulty string

Figure 3 shows a flowchart which classifies the various faults by ANN while using the percentage of linearity ratio calculation approach between the measured and simulated values for maximum power point current Impp and maximum power point voltage Vmpp.

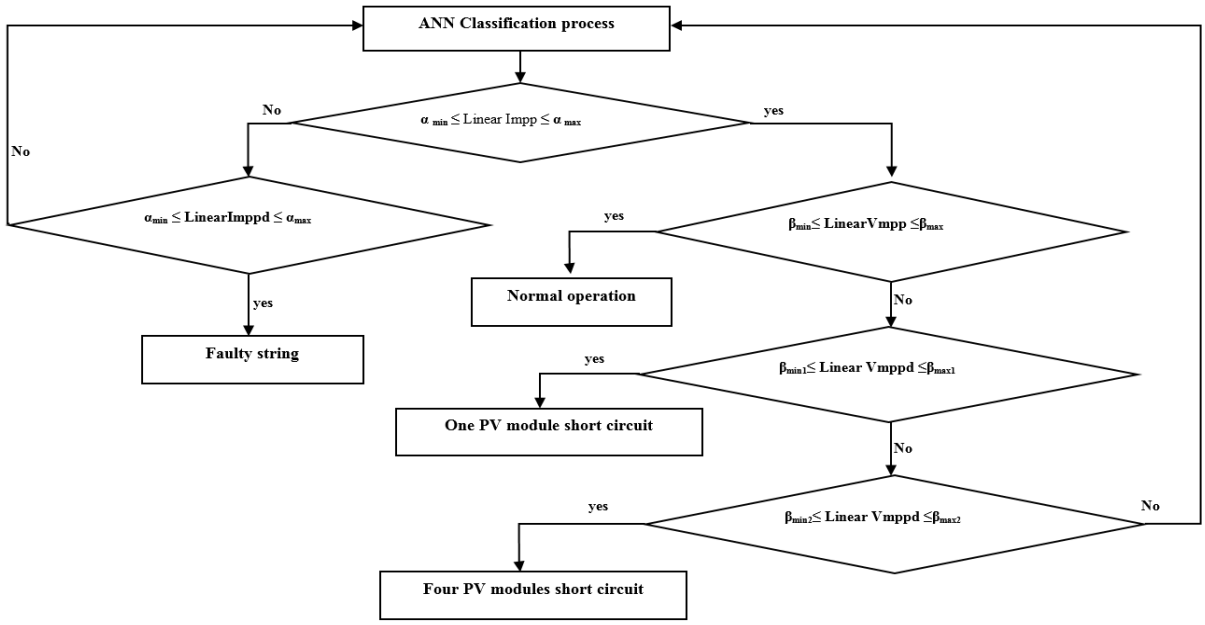

Figure 3. Proposed fault detection with Percentage of linearity

Table 5 shows the various minimum and maximum percentages of linearity ratio for all classification of faults.

TABLE V
PERCENTAGES OF LINEARITY RATIO

	α_{min} (%)	α_{max} (%)	β_{min} (%)	β_{max} (%)
Normal operation	95.36	101.67	98.43	101.59
1 PV Module Short Circuit	95.36	101.67	89.5	94.2
4 PV Module Short Circuit	95.36	101.67	47.24	57.41
Faulty string	49.41	52.77	98.43	101.59

D. *Approach based on ANN*

The simulation phase required 1000 simulated samples using MATLAB/Simulink for each case of variables Impp and Vmpp, 60% are used for training, 20% for validation and 20% for classification. In this study the architecture of ANN is multilayer perceptron (MLP), the transfer function used in this step is the sigmoid function. The approach required the Levenberg-Marquart algorithm for ANN training.

Step 1: called modelling requires five artificial neural networks for each case of classification of two variables Impp and Vmpp developed as follows:

- Selection of variable inputs.
- Data standardization.
- Selection of the network structure.
- Network training.
- Testing the network.

In this step, the network consisting of having two neurons in the input layer, one for the module temperature and the second for solar irradiance. One neuron for the output layer for each neural network representing Impp and Vmpp. The number of hidden layers is two for each neural network, each layer contains 9 x 12 neurons respectively [17].

Step 2: called classification requires two ANN, one for the classification of the Impp and the second for the classification of the Vmpp, these networks are developed in the same way as step 1. The simulation needs 20% of the remaining data of the Global dataset collected as well as 20% of the dataset provided by the ANN of step 1. The step 2 neural network consisting of having:

The first neural network: two neurons in the input layer corresponding to solar irradiance and measured maximum power point current and one neuron in the output layer representing Impp classification.

The second neural network: two neurons in the input layer corresponding to module temperature and measured maximum power point voltage and one neuron in the output layer representing Vmpp classification.

ISSN 2356-5608

The number of hidden layers is two for each neural network, each layer contains 8x8 neurons respectively.

V. RESULTS AND DISCUSSION

A. *Modelling*

The architecture of the neuron network for modelling Impp and Vmpp is shown in Figure 4:

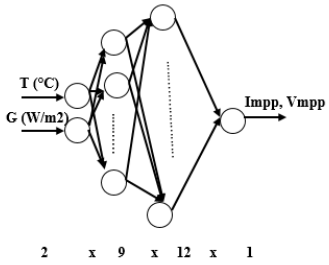

Figure 4- modelling ANN architecture

Figure 5 shows the learning graph which represent the Impp simulated versus Impp measured; the number of neurons in the input layer is two that represent the temperature and irradiance, the second graph represents the validation which refer to the Impp simulated versus Impp measured; this validation requires 300 dataset. The number of iterations is 1000, value epochs 0.0001, the RMSE of Impp normal operation and Impp faulty string is 0.6% and 0.58% respectively.

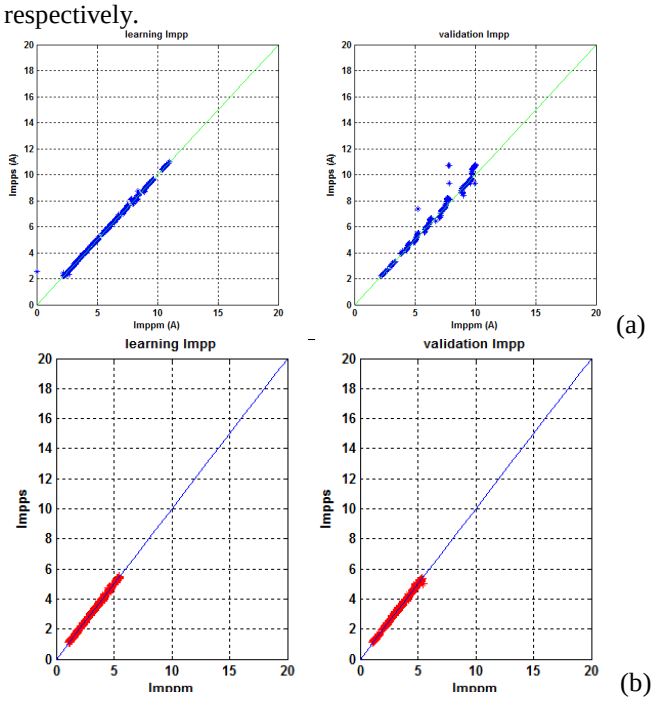

Figure 5- training and validation Impp (a) Normal operation, (b) Faulty string

The figure 6 shows the learning graph which represent the Vmpp simulated versus Vmpp measured; the second graph represents the validation which refer to the Vmpp simulated versus the Vmpp measured; we used 300 dataset. For Vmpp the number of iterations is 1000, epochs values are 0.0001, the RMSE of Vmpp normal operation, Vmpp of one PV module short circuit and Vmpp of four PV modules short circuit is 1.68% , 2.7% and 0.98% respectively.

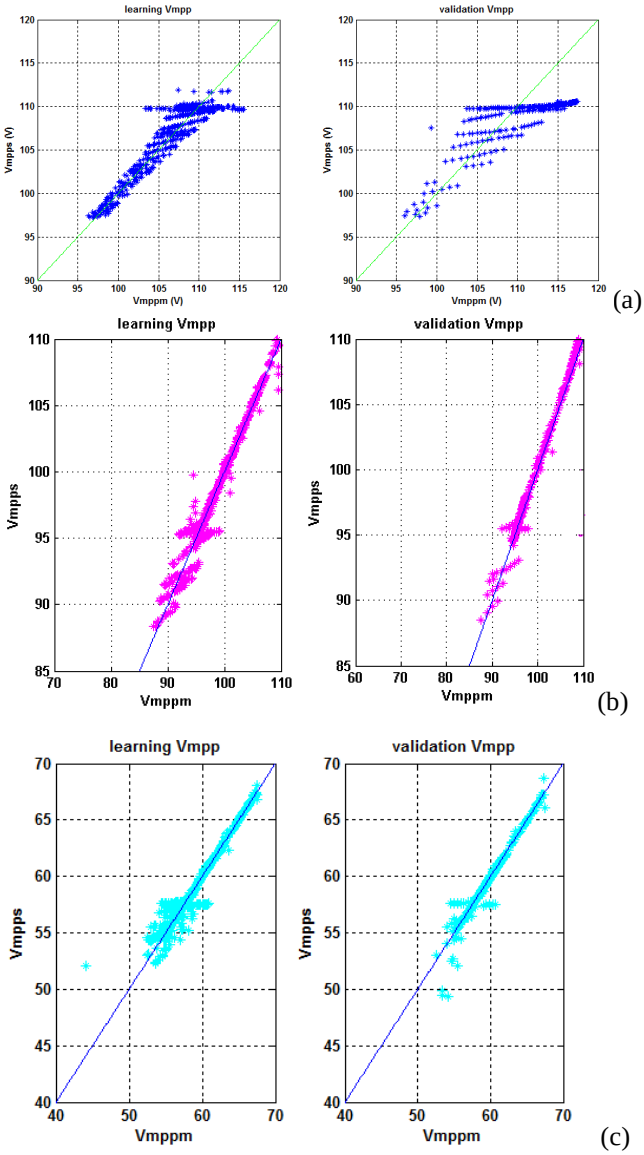

Figure 6- training and validation Vmpp (a) Normal Operation, (b) One PV module short circuit, (c) Four PV modules short circuit

Figure 7.a and 7.b represent the linear regression between the output of the network and its target, which explains the performance of the network, as for the perfect training the tangent would be 1, the correlation coefficient of Impp normal operation is 0.99091 and Vmpp normal operation is 0.95757.

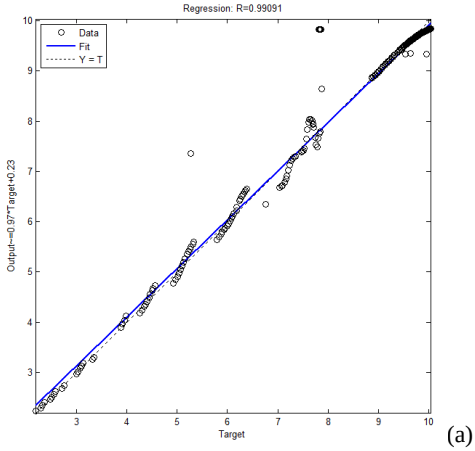

ISSN 2356-5608

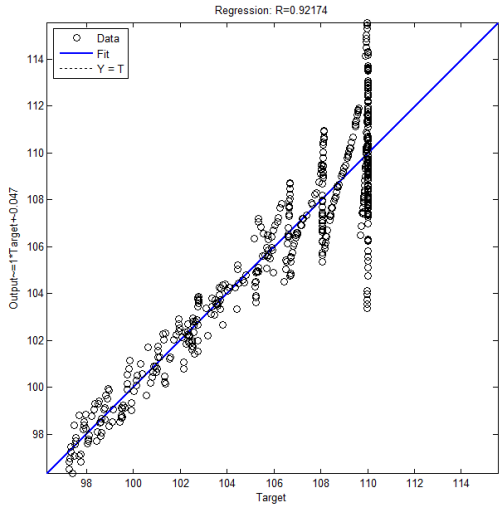

(b)

Figure 7- correlation coefficient (a) Impp , (b) Vmpp

B. *Detection and classification*

The architecture of the neuron network for classification Impp and Vmpp is shown in Figure 8:

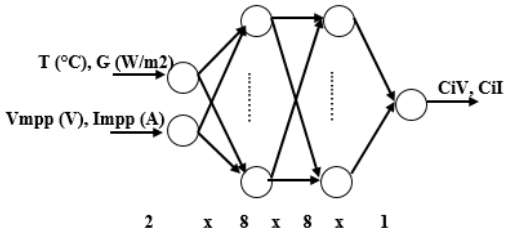

Figure 8- Classification ANN architecture

1) Detection

In normal operation case the measured of variables Impp and Vmpp must be linear to the simulated Impp and Vmpp by neural network around 100%, the data recorded are:

- 95.36% ≤ Impp ≤ 101.67%
- 98.43% ≤ Vmpp ≤ 101.59%

Beyond these percentage margins, the system begins to detect faults.

2) Classification

The system takes the variables Impp and Vmpp simulated by ANN from the normal operation system as a reference points to make the overall classification while calculating the minimum and the maximum percentage of linearity ration of each faults. A combinational algorithm of the percentage of linearity ratio is created to combines the percentage of the two variables Impp and Vmpp for the global classification. The system recorded the following percentages of linearity ratio:

One PV module short-circuit: 95.36%≤Impp≤101.67%
89.5%≤Vmpp≤94.2%

Four PV modules short-circuit: 95.36%≤Impp≤101.67%
47.24%≤Vmpp≤57.41%

Faulty string: 49.41%≤ Impp≤52.77%
98.43%≤Vmpp≤101.59%

Figure 9a and 9b show respectively the Impp measured versus Impp simulated and the Vmpp measured versus Vmpp simulated. Table 6 shows the various faults with their classification combinations where CiI represents the classification of the maximum current power point and CiV represents the classification of the maximum voltage power point.

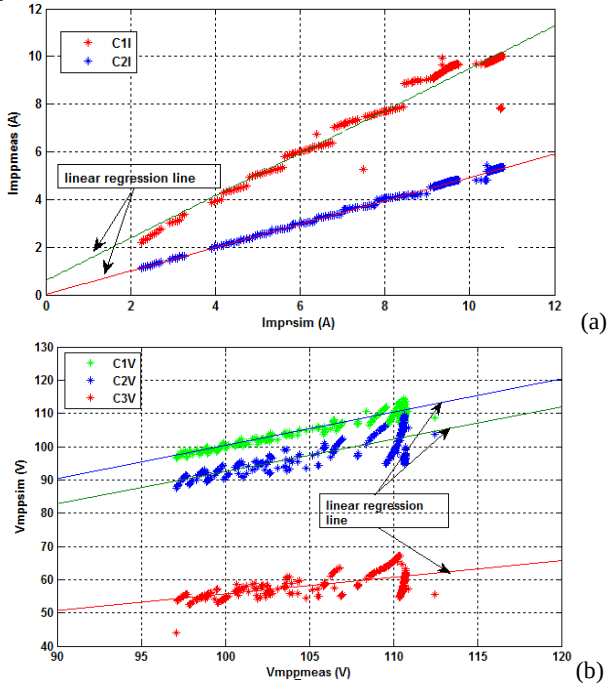

Figure 9- classification combination (a) Impp , (b) Vmpp

TABLE VV
TYPES OF FAULTS AND THEIR SYMBOLS

Types of faults	Symbols (Impp & Vmpp)
Normal operating	C1I & C1V
1PV Module short circuit	C1I & C2V
4 PV Module short circuit	C1I & C3V
Faulty string	C2I & C1V

VI. CONCLUSION:

This paper presents a new approach to the detection and classification of faults by artificial neural network (ANN) in a grid-connected photovoltaic system. The objective of this study was to propose a solution by taking less possible measured data to meet economic constraints.

Variables such as the current maximum power point and the voltage maximum power point measured (Impp-Vmpp) as well as simulated are compared for various faults.

The study was concluded by an experimental validation of the supervision strategy applied to the photovoltaic power plant connected to the CDER network, as well as the detection algorithm and the fault diagnosis. The results obtained confirm the ability to identify and classify various faults such as short-circuit and faulty string.

In the future, it is proposed to improve the detection and diagnostic capacity of large scale system experimentally in real time.

RÉFÉRENCES

[1] IEA, 2015. A Snapshot of Global PV Markets 2015. International Energy Agency (IEA)

[2] Potnuru, S.R., Pattabiraman, D., Ganesan, S.I., Chilakapati, N., 2015. Positioning of PV panels for reduction in line losses and mismatch losses in PV array. Renew. Energy 78, 264–275.

[3] Ishaque, K., Salam, Z., 2013. A review of maximum power point tracking techniques of PV system for uniform insolation and partial shading condition. Renew. Sustain. Energy Rev. 19, 475–488.

[4] Reisi, A.R., Moradi, M.H., Jamasb, S., 2013. Classification and comparison of maximum power point tracking techniques for

ISSN 2356-5608

photovoltaic system: a review. Renew. Sustain. Energy Rev. 19, 433–443.
[5] Marion, B., Schaefer, R., Caine, H., Sanchez, G., 2013. Measured and modelled photovoltaic system energy losses from snow for Colorado and Wisconsin locations. Sol. Energy 97, 112–121
[6] Tey, K.S., Mekhilef, S., 2014. Modified incremental conductance MPPT algorithm to mitigate inaccurate responses under fast-changing solar irradiation level. Sol. Energy 101, 333–342.
[7] Petruska, D.C., Stewart, D.K., Wegner, M.L., Eberhardt, G.M., 2015. U.S. Patent No. 8,931,457. U.S. Patent and Trademark Office, Washington, DC.
[8] Perpiñán, O., Marcos, J., Lorenzo, E., 2013. Electrical power fluctuations in a network of DC/AC inverters in a large PV plant: relationship between correlation, distance and time scale. Sol. Energy 88, 227–241.
[9] Takashima, T., Yamaguchi, J., Otani, K., Oozeki, T., Kato, K., Ishida, M., 2009. Experimental studies of fault location in PV module strings.Sol Energy Mater & Sol Cel, pp. 1079–1082.
[10] Solórzano, J., Egido, M.A., 2013. Automatic fault diagnosis in PV systems with distributed MPPT. Energy Convers. Manage. 76, 925–934.
[11] Chine.W., Mellit. A., Pavan,.A.M., Kalogirou. S.A., 2014. Fault detection method for grid-connected photovoltaic plants. Renew. Energy 66, 99–110.
[12] Platon, R., Martel, J., Woodruff, N., Chau, T.Y., 2015. Online fault detection in PV systems. IEEE Trans. Sustain. Energy 6 (4), 1200–1207.
[13] Chine, W., Mellit, A., Lughi, V., Malek, A., Sulligoi, G., Massi Pavan, A., 2016 .A novel fault diagnosis technique for photovoltaic systems based on artificial neural networks. Renew Energy 90 .501-512
[14] Chouder, A., Silvestre, S., Taghezouit, B., Karatepe, E., 2013. Monitoring, modelling and simulation of PV systems using LabVIEW. Sol. Energy 91, 337–349.
[15] Tadj, M., Benmouiza, K., Cheknane, A., Silvestre, S., 2014. Improving the performance of PV systems by fault detection using GISTEL approach. Energy Convers. Manage. 80, 298-304 .

ISSN 2356-5608